Electrochimica Acta 56 (2011) 7312–7318

Contents lists available at ScienceDirect

Electrochimica Acta

journal homepage: www.elsevier.com/locate/electacta

Evaluation of the hydrodynamic behaviour of turbulence promoters in parallel plate electrochemical reactors by means of the dispersion model

A.N. Colli, J.M. Bisang*

Programa de Electroquímica Aplicada e Ingeniería Electroquímica (PRELINE), Facultad de Ingeniería Química, Universidad Nacional del Litoral, Santiago del Estero 2829, S3000AOM Santa Fe, Argentina

ARTICLE INFO

Article history:
Received 29 March 2011
Received in revised form 17 May 2011
Accepted 15 June 2011
Available online 22 June 2011

Keywords:
Dispersion model
Electrochemical reactors
Hydrodynamic behaviour
Parallel plate electrodes
Turbulence promoters

ABSTRACT

The hydrodynamic behaviour of electrochemical reactors with parallel plate electrodes is experimentally studied using the stimulus-response method either with an empty reactor or with different turbulence promoters. Theoretical results which are in accordance with the analytical and numerical resolution of the dispersion model for a closed system are compared with the classical relationships of the normalized outlet concentration for open systems and the validity range of the equations is discussed. The experimental results were well correlated with the dispersion model using glass beads or expanded plastic meshes as turbulence promoters, which have shown the most advantageous performance. The Peclet number was higher than 63. The dispersion coefficient was found to increase linearly with flow velocity in these cases.

1. Introduction

Parallel plate electrochemical reactors are frequently used in the industrial practice and are recognized as a multipurpose device employed in a diverse range of electrochemical processes. One of the most common strategies to improve the performance of the reactors is the use of flow obstacles in the interelectrode gap to enhance the promotion of turbulence [1]. Thus, Cœuret and Storck [2] summarized the mass-transfer correlations for different turbulence promoters. In general, an important improvement in the mass-transfer coefficient is achieved depending on the type of promoter, its geometric dimensions and its orientation. Apart from this beneficial aspect of the turbulence promoters, they also modify the hydrodynamic behaviour of the electrochemical reactor, which requires some attention in its design.

Danckwerts [3] proposed a procedure for the study of the hydrodynamic behaviour in continuous flow systems, called stimulus-response method, in which the residence time distribution is determined by injecting an inert tracer into the vessel inlet and its concentration in the effluent stream is monitored versus time. Several signals can be used as a stimulus function, but the most common one is an instantaneous impulse in concentration at the vessel inlet, mathematically described as a Dirac delta function. The response function at the vessel outlet is processed in order to obtain the characteristic parameters of the models which have been proposed to represent the hydrodynamic behaviour of the equipment. In the last few years, a great number of works have been published concerning the implementation of the method, data acquisition, modelling, and ways to derive the model parameters from the residence time distribution data, which are properly summarized in [4,5]. In the case of electrochemical reactors with parallel-plate electrodes, hydrodynamic behaviour is frequently represented by the dispersion model. Thus, Jansson and Marshall [6,7] studied the axial dispersion in parallel-channel electrochemical cells under laminar flow conditions. A segregation of the flow near the wall was reported and the experimental results were reasonably correlated by an empirical model combining two axially dispersive plug flows. In [7] nitrogen was sparged into the system to simulate gas evolution at the electrodes, which drastically changes the mixing regime increasing the dispersion. The effect of electrogenerated gas bubbles on dispersion in the fluid close to the wall in a parallel-plate electrochemical reactor is reported in [8]. They corroborated that the dispersion coefficient increases with gas evolution at low liquid flow rates and it is unaffected at higher flow rates.

For a commercial filter-press reactor, the ElectroSyncell® cell, the axial dispersion is less significant when the frames contain the classical turbulence promoter instead of sheets of nickel foam [9]. However, hydrodynamics is always well described by a dispersed plug flow model and the Peclet number decreases whether the frames contain nickel foams or are empty. A study of flow

* Corresponding author.
E-mail address: jbisang@fiq.unl.edu.ar (J.M. Bisang).

0013-4686/$ – see front matter © 2011 Elsevier Ltd. All rights reserved.
doi:10.1016/j.electacta.2011.06.047

visualization for this reactor is reported in [10]. The hydrodynamic behaviour of the laboratory filter-press reactor, FM01-LC was extensively investigated [11–13]. It was found that the Peclet number shows a marked dependence on the turbulence promoter. Also, the flow pattern in a FM01-LC reactor strongly depends on the kind of turbulence promoter, entrance distributor geometry and channel thickness [14]. The effect of the ratio between felt and cell thicknesses in the hydrodynamic behaviour of a filter-press electrochemical reactor with carbon felt as a three-dimensional electrode was studied in [15]. Likewise, the flow dispersion measurements in the compartments of a modular 10 cell filter-press stack [16] showed that the reactor has two preferential paths for the electrolyte.

The aim of this work is to study the effect of turbulence promoters on the hydrodynamic behaviour of electrochemical reactors with parallel plate electrodes. Experimental results of residence time distributions obtained with the stimulus-response method are correlated according to the dispersion model to calculate the Peclet number.

2. Mathematical modelling

2.1. Analytical solution of the normalized concentration as a function of time for a closed system with Danckwerts' boundary conditions

The temporal behaviour of an electrochemical reactor without reaction according to the dispersion model is given by [17]

$$\frac{\partial c(T,y)}{\partial T} = \frac{1}{\mathrm{Pe}}\frac{\partial^2 c(T,y)}{\partial y^2} - \frac{\partial c(T,y)}{\partial y} \tag{1}$$

where

$$T = \frac{t}{\tau} \tag{2}$$

$$\tau = \frac{\varepsilon L}{u} \tag{3}$$

$$\mathrm{Pe} = \frac{uL}{\varepsilon D_L} \tag{4}$$

and

$$y = \frac{x}{L} \tag{5}$$

being c concentration (mol m^{-3}), Pe Peclet number, t time (s), τ space time (s), T dimensionless time, L electrode length (m), u mean superficial fluid velocity (m s^{-1}), ε porosity, D_L dispersion coefficient (m^2 s^{-1}), x axial coordinate (m) and y normalized axial coordinate, with the following initial and boundary conditions

$$T = 0; \quad c(0,y) = a\delta(y-0) \tag{6}$$

here a (mol m^{-3}) is a parameter defined by Eq. (12) and δ is the Dirac delta function,

$$y = 0 \text{ and } T > 0^+; \quad c(T,0) - \frac{1}{\mathrm{Pe}}\left.\frac{\partial c(T,y)}{\partial y}\right|_{y=0} = 0 \tag{7}$$

$$y = 1; \quad \left.\frac{\partial c(T,y)}{\partial y}\right|_{y=1} = 0 \tag{8}$$

Following the procedure outlined in [18] the solution of Eq. (1) is given by

$$c(T,y) = ae^{-(\mathrm{Pe}/4)T}e^{(\mathrm{Pe}/2)y}\sum_{n=1}^{\infty}\frac{2\lambda_n^2}{\lambda_n^2+\mathrm{Pe}^2/4+\mathrm{Pe}} \times \left[\cos(\lambda_n y) + \frac{\mathrm{Pe}}{2\lambda_n}\sin(\lambda_n y)\right] e^{-(\lambda_n^2 T/\mathrm{Pe})} \tag{9}$$

where λ_n are the positive roots in ascending order of the equation

$$tg(\lambda_n) = \frac{\lambda_n \mathrm{Pe}}{\lambda_n^2 - \mathrm{Pe}^2/4} \tag{10}$$

Evaluating Eq. (9) at $y = 1$, the outlet concentration for an impulse perturbation in the inlet concentration is given by

$$c(T,1) = ae^{\mathrm{Pe}/2}\sum_{n=1}^{\infty}\frac{2\lambda_n^2}{\lambda_n^2+\mathrm{Pe}^2/4+\mathrm{Pe}} \times \left[\cos(\lambda_n) + \frac{\mathrm{Pe}}{2\lambda_n}\sin(\lambda_n)\right] e^{-\left[(\mathrm{Pe}^2+4\lambda_n^2)/4\mathrm{Pe}\right]T} \tag{11}$$

The total mass of tracer introduced in the system is

$$\int_0^\infty c(T,1)\,dT = a \tag{12}$$

The normalized outlet concentration, called E curve [3], is given by

$$E(T) = \frac{c(T,1)}{\int_0^\infty c(T,1)dT} \tag{13}$$

Introducing Eqs. (11) and (12) into Eq. (13), taking into account Eq. (10), and rearranging results in

$$E(T) = 2e^{\mathrm{Pe}/2}\sum_{n=1}^{\infty}\frac{\lambda_n^2\cos(\lambda_n)(\lambda_n^2+\mathrm{Pe}^2/4)}{(\lambda_n^2+\mathrm{Pe}^2/4+Pe)(\lambda_n^2-\mathrm{Pe}^2/4)}e^{-\left[(\mathrm{Pe}^2+4\lambda_n^2)/4\mathrm{Pe}\right]T} \tag{14}$$

In [19,20], Eq. (1) was solved by assuming a negative step in concentration as an initial condition. Thus, in [19] Eq. (14) was obtained taking the first derivative of the concentration at the reactor outlet.

Applying the L'Hôspital's rule for $\mathrm{Pe} \to 0$, the terms in the summatory of order higher than one are zero and Eq. (14) approaches

$$E(T) = e^{-T} \tag{15}$$

valid for a continuous stirred tank electrochemical reactor.

2.2. Numerical solution of the normalized concentration as a function of time for a closed system with Danckwerts' boundary conditions

A numerical method to solve Eq. (1) is an attractive procedure because of the low rate of convergence of Eq. (14) for large values of Peclet number [21]. Thus, solving Eq. (1) with the implicit finite difference method [22] it is arrived to

$$c(T,y) = -\left(\frac{k}{2h} + \frac{k}{\mathrm{Pe}h^2}\right)c(T+k,y-h) + \left(\frac{2k}{\mathrm{Pe}h^2}+1\right)c(T+k,y) + \left(\frac{k}{2h} - \frac{k}{\mathrm{Pe}h^2}\right)c(T+k,y+h) \tag{16}$$

valid for $0 < T < \infty$ and $0 < y < 1$. Where h and k are the distance between two nodes in the y and t coordinates, respectively.

Likewise, at $y = 0$ is

$$c(T,0) = \left(1 + \frac{2k}{\mathrm{Pe}h^2} + k\mathrm{Pe} + \frac{2k}{h}\right)c(T+k,0) - \frac{2k}{\mathrm{Pe}h^2}c(T+k,0+h) \tag{17}$$

Analogously, at $y = 1$ is

$$c(T,1) = -\frac{2k}{\mathrm{Pe}h^2}c(T+k,1-h) + \left(\frac{2k}{\mathrm{Pe}h^2}+1\right)c(T+k,1) \tag{18}$$

and

$$c(0,0) = 1 \quad \text{and} \quad c(0,y) = 0 \quad \text{for } 0 < y \le 1 \tag{19}$$

The set of Eqs. (16)–(19) was solved by the tridiagonal matrix algorithm (TDMA) also known as Thomas algorithm [23]. It must

be emphasized that the numerical procedure represents a simple method for the calculation of concentration under different initial or boundary conditions.

2.3. Conventional equations of the normalized concentration as a function of time frequently used in electrochemical reactors

Solving Eq. (1) for an open system with the following initial and boundary conditions

$$T = 0; \quad c(0, y) = 0 \tag{20}$$

$$y = 0; \quad a\delta(T - 0) = \frac{c(T, 0)}{2} - \frac{1}{\mathrm{Pe}} \frac{\partial c(T, y)}{\partial y}\bigg|_{y=0} \tag{21}$$

$$y \to \infty; \quad (T, \infty) = 0 \tag{22}$$

it results

$$E(T) = \sqrt{\frac{\mathrm{Pe}}{4\pi T}} e^{-[\mathrm{Pe}(1-T)^2/4T]} \tag{23}$$

Eq. (21) considers that only half of the tracer enters into the reactor because in an open system it can diffuse in both positive and negative directions due to the initial concentration gradients [13]. Eq. (22) means that the system is not perturbed at a long distance from the reactor inlet and it retains the initial condition given by Eq. (20). Eq. (23) was given by Levenspiel and Smith [24].

Likewise, solving Eq. (1) for a semi-infinite dispersion system with the following initial and boundary conditions

$$T = 0; \quad c(0, y) = 0 \tag{24}$$

$$y = 0; \quad c(T, 0) = a\delta(T - 0) \tag{25}$$

$$y \to \infty; \quad c(T, \infty) = 0 \tag{26}$$

it results

$$E(T) = \sqrt{\frac{\mathrm{Pe}}{4\pi T^3}} e^{-[\mathrm{Pe}(1-T)^2/4T]} \tag{27}$$

Eq. (25) corresponds to the behaviour which is in accordance with the plug flow model, so that the dispersion is neglected at the reactor inlet. Eq. (27) was given by Gibilaro [25]. Eqs. (23) and (27) are frequently used to correlate experimental results in order to obtain the Peclet number [13].

3. Experimental

Fig. 1(a) shows a general diagram of the experimental setup. A vertical parallel plate electrochemical reactor, used in previous studies [26], was intercalated in a flow circuit system consisting of a pump, a flow meter, valves and thermostat. The reactor was made of acrylic material and both nickel electrodes had the same dimensions, 200 mm wide and 600 mm long. The solution flow in the reactor was upwards and in order to achieve a uniform distribution of electrolyte into the reactor, the inlet and the outlet reactor present an electrolyte manifold, denoted as (8) in Fig. 1. Six flexible connection sleeves joint the manifold to the flow distributor plate inside the reactor, which presents 116 holes, 1.5 mm in diameter. Thus, this special configuration of the distributor plates with numerous ports, symmetrically distributed, can minimize the dead zones in the corners of the reactor. To increase the mass transfer coefficient and to make it independent of the position in the reactor, the interelectrode gap, 13 mm, was completely filled with different turbulence promoters. Thus, three types of turbulence promoters were used, i.e.: woven plastic meshes, expanded plastic meshes and glass beads. The geometrical characteristics, measured in the laboratory and defined in Fig. 1(b) for the plastic expanded structure, are summarized in Table 1. In all cases the porosity was determined

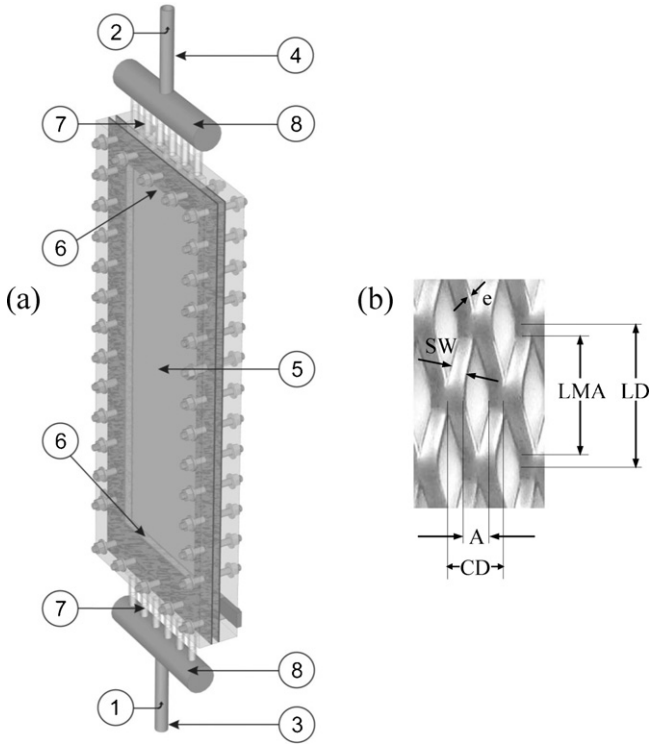

Fig. 1. (a) Schematic representation of the reactor. (1) Reactor inlet; (2) reactor outlet; (3) injection point; (4) measurement point; (5) reactor; (6) flow distributors; (7) connection sleeves; (8) inlet and outlet electrolyte manifolds. (b) View of the expanded plastic mesh with the characteristic parameters according to Table 1.

as the quotient between the volumes of water required to completely fill the interelectrode gap with and without the turbulence promoter. The experiments were performed at 30 °C.

Flow dispersion curves were obtained using the stimulus-response method. As a stimulus, an impulse function was simulated by manually injecting a 30 wt% NaOH solution, 0.2 cm^3, into the reactor inlet for a short time. Preliminary experiments were performed using an injection of a saturated KCl solution, but this alternative was rejected because it requires a higher volume, and consequently a higher injection time, to produce the same conductivity value at the reactor outlet. The electrolytic conductivity was monitored by means of a platinum conductivity cell formed by two parallel plate electrodes, WTW model LTA 01, with a cell constant 0.114 cm^{-1} mounted on a T-piece in the reactor outlet. The conductimeter was connected to a digital multimeter to obtain conductance versus time. It was verified that a linear relation between

Table 1
Geometrical parameters of the turbulence promoters.

Characteristic parameters of the expanded plastic mesh		
Long diagonal, LD		21.0 mm
Short diagonal, CD		5.5 mm
Long mesh aperture, LMA		12.5 mm
Short mesh aperture, *A*		3.0 mm
Thickness, *e*		1.2 mm
Apparent thickness (1 sheet)		2.4 mm
Strand width, SW		1.8 mm
Porosity		0.67
Characteristic parameters of woven mesh and glass beads	**Woven mesh**	**Glass beads**
Thread diameter or diameter (mm)	0.4	4
Mesh size (mm)	1.29 × 1.55	–
Porosity	0.72	0.4

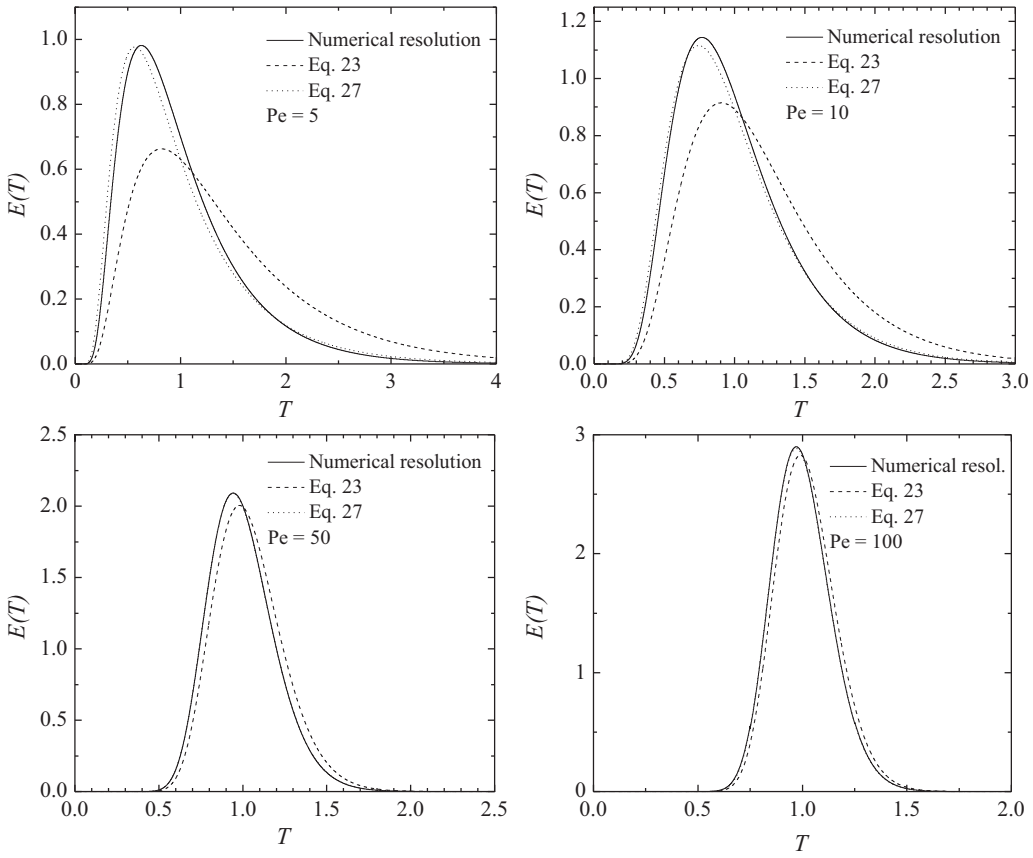

Fig. 2. Comparison of the response according to the numerical solution of Eq. (1) with those of Eqs. (23) and (27) at different Peclet numbers.

conductivity and concentration takes place in the measure range. To corroborate that the stimulus can be properly represented by the impulse function, in additional experiments, the concentration was measured close to the injection point and the data were fitted with a higher order polynomial. This equation was used in the numerical model as stimulus at the reactor inlet instead of the impulse function, Eq. (19). However, no significant difference was observed in both calculations.

4. Results and discussion

The calculations according to Eq. (14) for a number of eigenvalues higher than ten agree with those of the numerical resolution of Eq. (1) and both calculation procedures are comparable. However, for large values of Peclet number the numerical method is more convenient due to the inadequate convergence of the analytical solution.

Fig. 2 compares the temporary response of the normalized concentration for a closed system with Danckwerts' boundary conditions with those given by Eqs. (23) and (27). It is observed that for a Peclet number of 5 the equations show discrepancy. However, for Pe higher than 10, Eq. (27) agrees with the analytical or numerical solution of the closed system and all the calculation procedures present the same performance when the Peclet number is very high.

In the following experimental data, each curve represents the smoothed values of five independent experiments and a dimensionless time referred to the mean residence time, t_{mean} (s), was used, which was calculated as

$$t_{mean} = \frac{\int_0^\infty tc(t)\,dt}{\int_0^\infty c(t)\,dt} \quad (28)$$

Thus, the curves in Fig. 3 show the change of the normalized outlet concentration at different flow rates of the electrolyte, Q ($m^3\,s^{-1}$), for the reactor without turbulence promoters. A main peak and a pronounced tail can be observed, which is more prominent at the lower value of volumetric flow rate. Due to the special configuration of the flow distributors at the inlet and outlet of the reactor, the existence of dead zones inside the equipment can be disregarded and the tail can be attributed to the slow flow near the electrodes. Fig. 3 also shows that all the curves are overlapped at volumetric

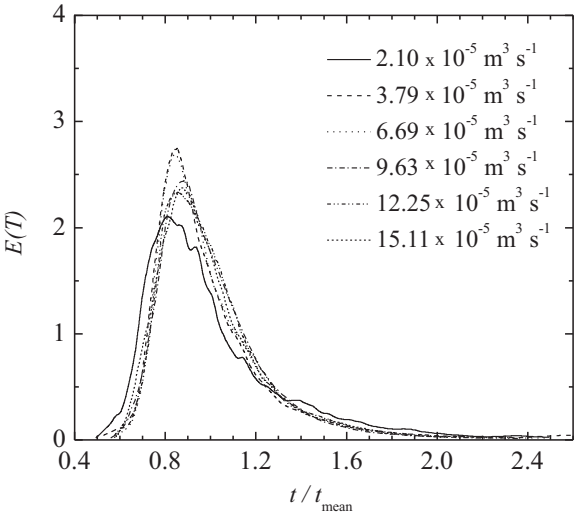

Fig. 3. Experimental residence time distribution for the reactor without turbulence promoters.

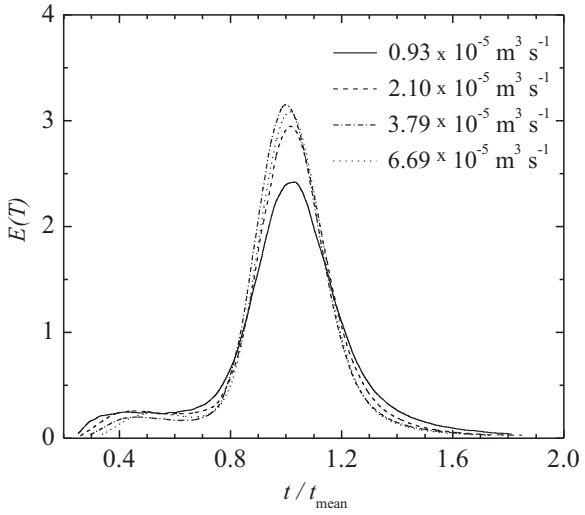

Fig. 4. Experimental residence time distribution parametric in volumetric flow rate. Woven plastic meshes as turbulence promoters.

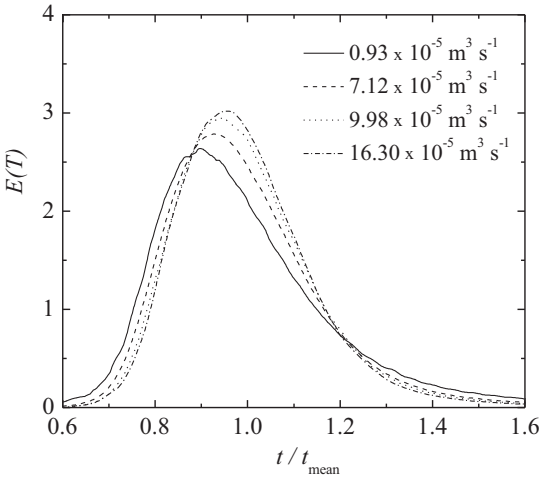

Fig. 5. Experimental residence time distribution parametric in volumetric flow rate. Expanded plastic meshes as turbulence promoters.

Table 2
Summary of results using woven plastic meshes as turbulence promoter.

$Q \times 10^5$ ($m^3\ s^{-1}$)	τ (s)	t_{mean} (s)	*P*-value	$\Delta p/\Delta s$	Peak-abscissae
0.93	140.32	143.85	0.36	9.82	1.024
2.10	62.42	62.50	0.97	10.61	1.017
3.79	34.59	35.14	0.14	14.88	1.002
6.69	19.58	20.11	0.12	13.08	1.01
9.63	13.61	13.75	0.25	14.12	1.002
12.25	10.69	10.59	0.52	16.28	0.999
15.11	8.67	8.52	0.13	16.01	0.994

flow rates higher than $12.25 \times 10^{-5}\ m^3\ s^{-1}$. In these experiments the space time was higher than the mean residence time. In some experiments one of the plate electrodes was replaced by a flattened expanded metal sheet of the same dimensions. However, no change in the reactor performance was observed.

To avoid the slow flow zones inside the reactor, turbulence promoters were incorporated in the interelectrode gap. Fig. 4 shows some typical results of the performance of the reactor with the interelectrode gap filled with a stack 16 sheets of woven plastic meshes. At higher volumetric flow rates the data are overlapped. The curves of the normalized outlet concentration as a function of the dimensionless time show a shoulder at short times, which can be attributed to the formation of by-pass channels in the stack of plastic meshes. Thus, two phases can be identified in the solution flow: a fast phase and a slow one, the latter generates the main peak in the curves. A similar behaviour was reported in [13]. In all these experiments the space time was in close agreement with the mean residence time, second and third columns of Table 2 respectively, which is corroborated by the value of the statistical parameter, *P*-value [27], higher than 0.05 given in the fourth column. Likewise, the last two columns in Table 2 report the ratio of the heights between the peak and the shoulder, $\Delta p/\Delta s$, and the abscissae of the peaks respectively. The ratio $\Delta p/\Delta s$ increases when the volumetric flow rate increases, its value is strongly dependent on the packaging of the meshes but the same tendency was observed in all cases. Thus, the channelling decreases at high volumetric flow rates and at the same time the position of the peaks is shifted to shorter times approaching 1. Therefore, in comparison with the empty reactor, the presence of a stack of woven plastic meshes restricts the slow zones near the electrodes but generates the channelling of flow as a detrimental aspect.

Fig. 5 shows typical results using plastic meshes as turbulence promoters, which present a configuration similar to expanded structures. Thus, the interelectrode gap was filled with six sheets of expanded plastic mesh. Likewise, Fig. 6 shows the results from glass beads as turbulence promoters. In Figs. 5 and 6, it can be observed that the use of expanded plastic meshes or glass beads eliminates the flow channelling and also reduces the tail at higher times

Table 3
Summary of results using expanded plastic meshes or glass beads as turbulence promoter.

Turbulence promoter	$Q \times 10^5$ ($m^3\ s^{-1}$)	τ (s)	t_{mean} (s)	*P*-value	Numerical solution of Eq. (1)		Eq. (23)		Eq. (27)	
					Pe	MSE	Pe	MSE	Pe	MSE
Expanded plastic meshes	0.93	130.68	140.70	0.06	62 ± 2	0.1385	63 ± 3	0.2907	63 ± 2	0.1373
	2.10	58.14	61.08	0.14	89 ± 3	0.1176	90 ± 4	0.2476	90 ± 2	0.1161
	3.79	32.21	33.06	0.26	93 ± 3	0.1180	93 ± 4	0.2449	93 ± 3	0.1166
	7.12	17.14	17.68	0.39	80 ± 2	0.0677	81 ± 3	0.1884	81 ± 2	0.0666
	9.98	12.23	11.88	0.09	94 ± 2	0.0460	95 ± 3	0.1501	95 ± 2	0.0449
	13.04	9.36	9.43	0.73	100 ± 2	0.0397	100 ± 4	0.1371	100 ± 2	0.0387
	16.30	7.47	7.59	0.37	102 ± 2	0.0507	103 ± 4	0.1512	103 ± 2	0.0496
Glass beads	0.93	87.83	89.15	0.649	75 ± 2	0.0531	76 ± 3	0.1640	76 ± 2	0.0526
	2.10	39.08	40.26	0.156	108 ± 2	0.0347	109 ± 4	0.1287	109 ± 2	0.0341
	3.79	21.65	21.65	0.990	128 ± 2	0.0275	128 ± 4	0.1140	128 ± 2	0.0270
	6.69	12.25	13.08	0.081	148 ± 2	0.0342	149 ± 4	0.1207	149 ± 3	0.0336
	9.63	8.52	8.37	0.743	164 ± 3	0.0417	163 ± 6	0.1300	164 ± 3	0.0410
	12.25	6.69	6.67	0.628	163 ± 4	0.0513	162 ± 7	0.1417	164 ± 4	0.0505
	15.11	5.43	5.50	0.313	164 ± 7	0.1062	162 ± 10	0.2242	164 ± 6	0.1051

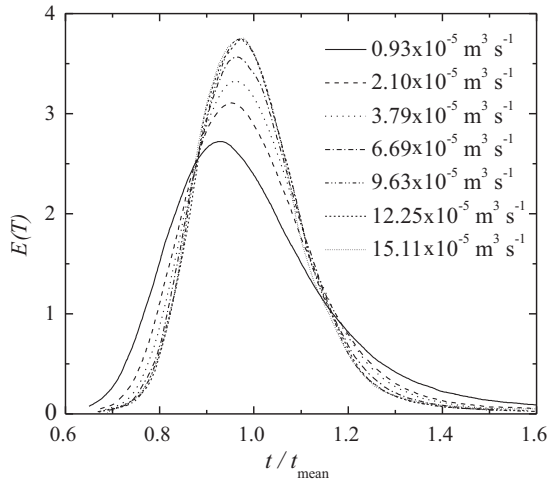

Fig. 6. Experimental residence time distribution parametric in volumetric flow rate. Glass beads as turbulence promoters.

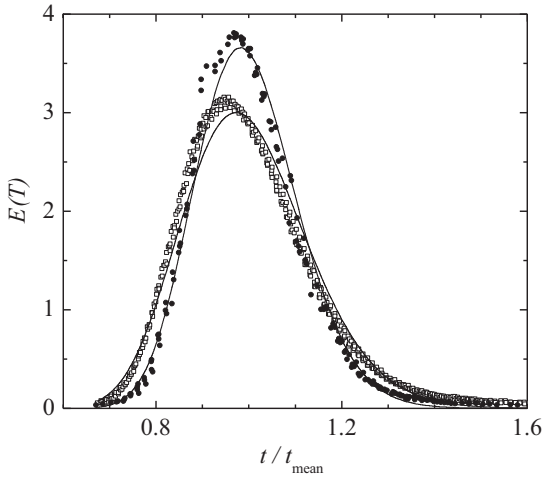

Fig. 8. Residence time distribution. Glass beads as turbulence promoters. *Open square*: $Q = 2.10 \times 10^{-5}$ m^3 s^{-1}. *Full circle:* $Q = 12.25 \times 10^{-5}$ m^3 s^{-1}. Continuous lines: correlation according to Eq. (27).

observed in the empty reactor. Likewise, the experimental data are overlapped at high volumetric flow rates. These experimental data were correlated by means of a weighted least square method applied to Eq. (27) and using the Peclet number as fitting parameter. Figs. 7 and 8 compare some experimental data with their correlation results. To quantify the agreement between theoretical and experimental data, the mean square error is introduced as

$$\mathrm{MSE} = \frac{1}{N-1}\sum_{i=1}^{N}\gamma_i(E_i^{\mathrm{th}} - E_i^{\mathrm{exp}})^2 \tag{29}$$

where N is the number of experimental data and the subscripts "exp" and "th" denote the experimental and theoretical values, respectively, the weighted factor is given by

$$\gamma_i = \frac{E_i^{\mathrm{exp}}}{E_{\mathrm{mean}}^{\mathrm{exp}}} \tag{30}$$

The Peclet number for which MSE is minimal is then taken as the best fit value. Table 3 summarizes the results.

The high value of the P-value corroborates the agreement between the space time and the mean residence time, third and fourth columns of Table 3 respectively. In Figs. 5 and 6, the displacement of the peak towards $T = 1$ when the volumetric flow rate increases can be attributed to the increase in the Peclet number as reported in Table 3, where the values for a 95% confidence interval are given. Thus, the last six columns of this table compare the correlation of the experimental results according to the numerical solution of Eq. (1) with those of Eqs. (23) and (27), where the Peclet number and the mean square error are reported. It can be concluded that all the equations yield Peclet numbers in the same confidence interval. However, in accordance with Fig. 2, the numerical solution and Eq. (27) show similar values of the mean square error, which are better than those obtained with Eq. (23). The Peclet values given in Table 3 are similar to those reported in [12] for the FM01-LC electrochemical reactor with polyester open-cell foams. The high values of the Peclet number approach the behaviour of this reactor with glass beads as turbulence promoters to that of the plug flow model. Thus, taking into account Figs. 3–8 it can be concluded that all the detrimental aspects for the hydrodynamic behaviour, such as presence of tails, by-passes or dead zones can be avoided as long as the inlet and the outlet of the electrolyte are well designed and the turbulence promoter is properly chosen. Fig. 9 reports that the axial dispersion coefficient divided by the kinematic viscosity, ν (m^2 s^{-1}), increases linearly with the Reynolds number for both turbulence promoters, expanded plastic meshes and glass beads. The Reynolds number was calculated as $d_e u/\nu$, here d_e (m) is the

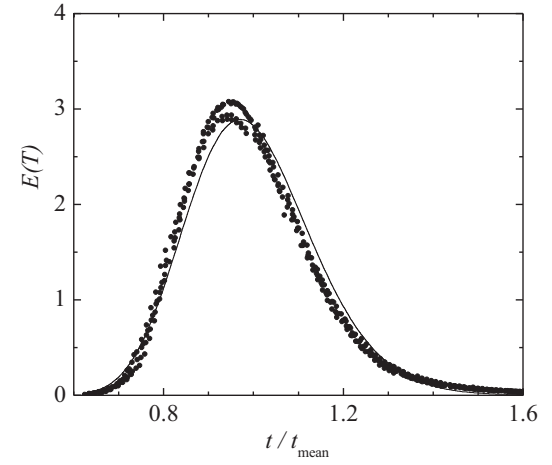

Fig. 7. Residence time distribution. Expanded plastic meshes as turbulence promoters. *Full circle:* experimental data. Continuous lines: correlation according to Eq. (27). $Q = 12.25 \times 10^{-5}$ m^3 s^{-1}.

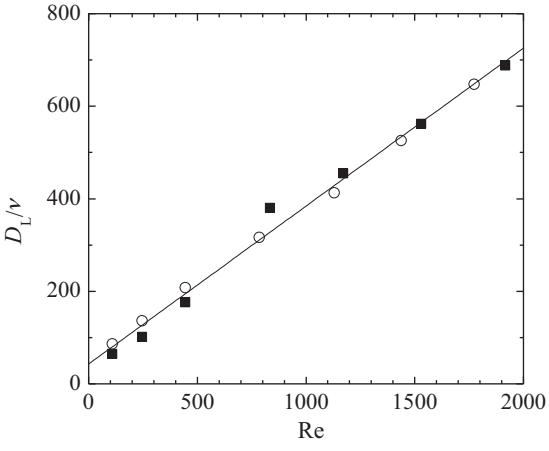

Fig. 9. Dispersion coefficient divided by the kinematic viscosity as a function of the Reynolds number. *Full square*: Expanded plastic meshes as turbulence promoters. *Open circle:* Glass beads as turbulence promoters.

hydraulic diameter of the channel defined as $2w_c d_c/(w_c + d_c)$; being d_c (m) the interelectrode gap and w_c (m) the width of the reactor. The same tendency was reported in [11] for the FM01-LC reactor in spite of their different geometric configuration.

5. Conclusions

- For Peclet numbers higher than 10 the solution of Eq. (1) for a closed system with Danckwerts' boundary conditions gives the same result that Eq. (27) and for Pe values higher than 50 all the calculation procedures show similar performance.
- It was corroborated that the hydrodynamic behaviour of an electrochemical reactor with parallel plate electrodes is strongly dependent on the nature of the turbulence promoter. Thus, for the choice of a suitable turbulence promoter it is necessary to take into account materials with good mass-transfer conditions and also with an appropriate hydrodynamic behaviour.
- The hydrodynamic behaviour can be represented by the dispersion model, with high values of Peclet number, if glass beads or expanded plastic meshes are used as turbulence promoters. Likewise, from the hydrodynamic point of view these promoters show the more advantageous performance.
- In a parallel plate electrochemical reactor with expanded plastic meshes or glass beads as turbulence promoters, the axial dispersion coefficient increases linearly with the volumetric flow rate.

Acknowledgements

This work was supported by the Agencia Nacional de Promoción Científica y Tecnológica (ANPCyT), Consejo Nacional de Investigaciones Científicas y Técnicas (CONICET) and Universidad Nacional del Litoral (UNL) of Argentina.

References

[1] D. Pletcher, F.C. Walsh, Industrial Electrochemistry, Chapman and Hall, London, 1993, pp. 146–155 (Chapter 2).
[2] F. Cœuret, A. Storck, Elements de Genie Electrochimique, TEC&DOC, Paris, 1984, pp. 148–155 (Chapter 3b).
[3] P.V. Danckwerts, Chem. Eng. Sci. 2 (1953) 1.
[4] K.R. Westerterp, W.P.M. van Swaaij, A.A.C.M. Beenackers, Chemical Reactor Design and Operation, John Wiley & Sons, New York, 1987 (Chapter IV).
[5] H. Scott Fogler, L.F. Brown, Elements of Chemical Reaction Engineering, 4th ed., Prentice Hall, New Jersey, 2005 (Chapters 13 and 14).
[6] R.J. Marshall, R.E.W. Jansson, J. Chem. Technol. Biotechnol. 30 (1980) 359.
[7] R.E.W. Jansson, R.J. Marshall, Electrochim. Acta 27 (1982) 823.
[8] W.S. Wu, G.P. Rangaiah, M. Fleishmann, J. Appl. Electrochem. 23 (1993) 113.
[9] A. Montillet, J. Comiti, J. Legrand, J. Appl. Electrochem. 23 (1993) 1045.
[10] C. Bengoa, A. Montillet, P. Legentilhomme, J. Legrand, J. Appl. Electrochem. 27 (1997) 1313.
[11] P. Trinidad, F.C. Walsh, Electrochim. Acta 41 (1996) 493.
[12] C. Bengoa, A. Montillet, P. Legentilhomme, J. Legrand, Ind. Eng. Chem. Res. 39 (2000) 2199.
[13] P. Trinidad, C. Ponce de León, F.C. Walsh, Electrochim. Acta 52 (2006) 604.
[14] F.F. Rivera, M.R. Cruz-Díaz, E.P. Rivero, I. González, Electrochim. Acta 56 (2010) 361.
[15] J. González-García, V. Montiel, A. Aldaz, J.A. Conesa, J.R. Pérez, G. Codina, Ind. Eng. Chem. Res. 37 (1998) 4501.
[16] C. Ponce de León, I. Whyte, G.W. Reade, S.E. Male, F.C. Walsh, Aust. J. Chem. 61 (2008) 797.
[17] K. Scott, Electrochemical Reaction Engineering, Academic Press, London, 1991, p. 291 (Chapter 5).
[18] J.M. Bisang, J. Appl. Electrochem. 38 (2008) 161.
[19] S. Yagi, T. Miyauchi, Kagaku Kogaku 17 (1953) 382.
[20] T. Otaka, E. Kunigita, Kagaku Kogaku 22 (1958) 144.
[21] A.D. Martin, Chem. Eng. Sci. 55 (2000) 5907.
[22] S.C. Chapra, R.P. Canale, Numerical Methods for Engineers, 5th ed., McGraw-Hill, New York, 2006, p. 845 (Chapter 30).
[23] S.D. Conte, C.W. de Boor, Elementary Numerical Analysis: An Algorithmic Approach, 3rd ed., McGraw-Hill, New Auckland, 1980, p. 153 (Chapter 4.2).
[24] O. Levenspiel, W.K. Smith, Chem. Eng. Sci. 6 (1957) 227.
[25] L.G. Gibilaro, Chem. Eng. Sci. 33 (1978) 487.
[26] J.M. Bisang, J. Appl. Electrochem. 27 (1997) 379.
[27] D.C. Montgomery, G.C. Runger, Applied Statistics and Probability for Engineers, 3rd ed, John Wiley & Sons, New York, 2003, p. 292 (Chapter 9).